HHS Public Access

Author manuscript

*J Bone Miner Res*. Author manuscript; available in PMC 2015 December 01.

Published in final edited form as:

*J Bone Miner Res*. 2014 December ; 29(12): 2653–2665. doi:10.1002/jbmr.2287.

# Runx2 Regulates Endochondral Ossification through Control of Chondrocyte Proliferation and Differentiation

**Haiyan Chen, PhD**, **Farah Y. Ghori-Javed, MD**, **Harunur Rashid, MSc**, **Mitra D. Adhami, BS**, **Rosa Serra, PhD**[*], **Soraya E. Gutierrez, PhD**[#], and **Amjad Javed, PhD**

[*]Department of Oral and Maxillofacial Surgery and Cell, Developmental and Integrative Biology. Institute of Oral Health Research, School of Dentistry, University of Alabama at Birmingham, Alabama

[#]Departamento de Bioquimica y Biología Molecular, Universidad de Concepción, Concepción, Chile

## Abstract

Synthesis of cartilage by chondrocytes is an obligatory step for endochondral ossification. Global deletion of the Runx2 gene results in complete failure of the ossification process, but the underlying cellular and molecular mechanisms are not fully known. Here, we elucidated Runx2 regulatory control distinctive to chondrocyte and cartilage tissue by generating Runx2 exon 8 floxed mice. Deletion of Runx2 in chondrocytes caused failure of endochondral ossification and lethality at birth. The limbs of $Runx2^{\Delta E8/\Delta E8}$ mice were devoid of mature chondrocytes, vasculature, and marrow. We demonstrate that the C-terminus of Runx2 drives its biological activity. Importantly, nuclear import and DNA binding functions of Runx2 are insufficient for chondrogenesis. Molecular studies revealed that despite normal level of Sox9 and PTHrP, chondrocyte differentiation and cartilage growth is disrupted in $Runx2^{\Delta E8/\Delta E8}$ mice. Loss of Runx2 in chondrocytes also impaired OPG-RANKL signaling and chondroclast development. Dwarfism observed in Runx2 mutants was associated with the near absence of proliferative zone in the growth plates. Finally, we show Runx2 directly regulates a unique set of cell cycle genes Gpr132, Sfn, c-Myb, and Cyclin A1 to control proliferative capacity of chondrocyte. Thus, Runx2 is obligatory for both proliferation and differentiation of chondrocytes.

### Keywords

Runx2; Chondrocyte differentiation; Skeletal development; Cartilage remodeling

Corresponding author: Amjad Javed Ph.D., Department of Oral and Maxillofacial Surgery, School of Dentistry SDB 714, University of Alabama at Birmingham, 1720 2ND Avenue South, Birmingham, AL 35294-0007, (205) 996-5124 (phone), (205) 934-1560 (fax), javeda@uab.edu.

**Authors' role**s: Study design: AJ. Study conduct: AJ, HC, FG-J, HR and MA. Data collection: AJ, HC, FG-J, HR and MA. Data analysis: AJ, HC, FG-J, HR, MA, SG and RS. Data interpretation: AJ, HC, FG-J, HR, MA, SG and RS. Drafting manuscript: AJ, HC, FG-J, HR, MA, RS and SG. AJ take responsibility for the integrity of the data analysis.

## Introduction

During skeletal development, the appendicular and part of the axial skeletons are formed largely by endochondral ossification. This intricate process involves the formation of a cartilage anlagen, which is later resorbed and replaced by mineralized bone (1). Based on their location and morphology in the growth plate, chondrocytes are classified into resting, proliferative, prehypertrophic and hypertrophic zones. The process of unidirectional chondrocyte differentiation is also characterized by the expression of zone specific marker genes (2). Terminally mature hypertrophic chondrocytes contribute to cartilage calcification, undergo apoptosis, and are replaced by bone-forming osteoblasts (2,3). This intricate process of chondrogenesis in the growth plate continues until skeletal maturity during postnatal endochondral ossification.

Two ligands secreted by chondrocytes, parathyroid hormone-related protein (PTHrP) and indian hedgehog (Ihh), are key regulators of chondrogenesis and endochondral ossification. PTHrP and Ihh act in a regulatory loop to promote chondrocyte proliferation. Ihh secreted from prehypertophic chondrocytes induces the expression of PTHrP in the periarticular region to promote chondrocyte proliferation (4). Ihh-null chondrocytes do not express PTHrP (5). On the other hand, PTHrP suppresses Ihh expression via a negative feedback loop to delay chondrocyte hypertrophy (6,7). Deletion of either Ihh or PTHrP gene results in shortened limbs due to accelerated hypertrophy and poor chondrocyte proliferation (7,8). However, chondrocytes undergo hypertrophy in both the Ihh and PTHrP null mice, indicating involvement of additional pathways (9,10). Indeed, TGF-β/BMPs, FGF, and Wnt/β-catenin pathways function in conjunction with Ihh signaling to regulate chondrocyte differentiation (11–14).

Members of the Sox transcription factor family are essential for chondrogenesis. Sox9 starts expressing in mesenchymal cells prior to condensation in all developing skeletal elements and continues to express during sequential steps of chondrocyte differentiation (15,16). Haploinsufficiency of Sox9 results in lethality and chondrocyte specific deletion of Sox9 causes failed chondrogenesis (15). Sox9 directly regulates expression of markers for proliferating and hypertrophic chondrocytes (16,17). Sox5 and Sox6 are also expressed during chondrocyte differentiation, but unlike Sox9, are not required for mesenchymal condensation. Both Sox5 and Sox6 are downstream of Sox9 and deletion of either gene shows mild defect in endochondral ossification (18). Among the Sox trio, only Sox9 is required for expression of Ihh and PTHrP in chondrocytes (15,18). The disrupted PTHrP-Ihh regulatory loop is a critical component of failed chondrogenesis noted in Sox9 null mice (15,18).

The runt-related transcription factor 2 (Runx2) is a member of the Runx gene family necessary for organogenesis and survival. Runx2 is widely known for its essential role during commitment and differentiation of mineralizing cell types. Global deletion of Runx2 results in disrupted chondrocyte and osteoblast differentiation and complete loss of skeletal mineralization, indicating a regulatory role of Runx2 in both cell types (19–21). Runx2 expression in prehypertrophic chondrocytes is required to promote chondrocyte hypertrophy

(22,23). Thus, unlike Sox9, which initiates chondrogenesis, Runx2 is generally considered as a major driver for the later stages of endochondral ossification (15,17,22–25).

During skeletogenesis, Runx2 is expressed in both chondrocytes and osteoblasts, but global null models are unable to distinguish the cell-specific functions of Runx2. Misexpression approaches have failed to define the chondrocyte-specific roles of Runx2. Overexpression of Runx2 in developing chondrocytes by the Col IIa promoter results in accelerated chondrocyte maturation, ectopic ossification of cartilage, and lethality at birth (23). However, another group has reported a mixed phenotype, with some Col IIa-Runx2 transgenic mice dying at birth, while other transgenic mice survive and exhibit normal skeletal growth (22). These variations in endochondral ossifications are linked to the level of Runx2 being overexpressed in chondrocytes. Interestingly, blockage of endogenous activity of all Runx family members by overexpression of dominant negative forms of Runx2 in chondrocytes results in lethality due to failed endochondral ossification (23). In sharp contrast, no skeletal phenotype was noted in independent transgenic lines where a similar dominant negative form of Runx2 was overexpressed in chondrocytes (22). Moreover, overexpression of Runx2 in hypertrophic chondrocytes only causes a mild decrease in ossification of selected digits (26). The Col Xa-Runx2 transgenic mice have a normal life span and comparable skeleton to wild type mice (26). Thus, due to contradictory phenotypes, the specific contribution of endogenous Runx2 in chondrocytes remains unclear. Surprisingly, conditional ablation of the Runx2 gene in chondrocyte with Col IIa-Cre leads to perinatal lethality and failed endochondral ossification (27,28). Interestingly, similar phenotype is noted with deletion of either N-terminal (exon 4) or C-terminal (exon 8) region of Runx2. However, the underlying mechanisms responsible for loss of endochondral ossification in these models are yet to be studied. Here we demonstrate that C-terminus of Runx2 is obligatory for both proliferation and terminal differentiation of chondrocyte.

## Materials and Methods

### Generation of Runx2 conditional knockout mice

To generate Runx2 exon 8 floxed mice, targeting vectors harboring a directional loxP site, a floxed neomycin gene, and a thymidine kinase gene were generated. A step wise cloning strategy involving five intermediate vectors was used to assemble pTLNLoxP the final targeting vector (see supplement methods). The correctness of the targeting construct was confirmed by restriction digestion and sequence analysis (Fig 1B). The linearized targeting vector was electroporated into mouse ES cells. The integrity of the targeted locus in positive ES cells was confirmed by southern blot analysis using 5′ and 3′ external probes. The positive ES cells underwent a second round of selection to identify cells where the Neomycin gene has been removed and the Runx2 allele is floxed (Fig S2A & supplement methods). Two independent ES clones with the floxed Runx2 allele were used for blastocyst injection to generate chimeras. The chimeric animals were bred with C57/BL6 mice to confirm germ line transmission of the ES cells. The heterozygous ($Runx2^{+/F}$) mice were intercrossed to obtain homozygous ($Runx2^{F/F}$) floxed animals and genotypes were confirmed by PCR analysis using primers described in Table S1. To delete Runx2 in

chondrocyte, mice were crossed with Col IIa-Cre mice (27,29). Expression of Cre recombinase in chondrocyte and cartilage tissue was confirmed with Rosa26 reporter line (30). All animal experiments were performed with the approval of the Animal Research Program of the University of Alabama at Birmingham and conformed to relevant federal guidelines.

### Skeletal staining and histological analysis

Skeletal preparations from embryonic, new born and postnatal mice were double stained with alcian blue and alizarin red to assess skeletogenesis and are described in supplement methods. For histological analysis, new born and E18.5 embryos were fixed overnight in 4% paraformaldehyde (Sigma-Aldrich, St. Louis, MO). Tibia and femur were dehydrated in gradient ethanol, embedded in paraffin and sectioned at 7μm thickness. Tissue sections were dewaxed in xylene, rehydrated in gradient ethanol and processed for hematoxylin and eosin, alcian blue, and TRAP staining as described in supplement methods. Detailed procedure for BrdU, Sox9, CD31 and Caspase 3 immunohistochemistry and in situ hybridization for Col Xa is described in supplement methods.

### RNA and western blot analysis

Total RNA was extracted from axial and appendicular skeletons from embryonic and new born mice using Trizol reagent (Invitrogen Inc, CA). The prepared cDNA was used for quantitative real-time PCR (q-PCR) performed with iQ SYBR Green Supermix (Bio-Rad Hercules, CA). Gene specific primers are listed in Table S2. The cell cycle gene profiles were assessed using Mouse Cell Cycle RT$^2$ Profiler™ PCR array system (Qiagen, Valencia, CA). The expression values were normalized with 5 housekeeping genes and relative expression of each target gene was calculated by RT$^2$ Profiler™ PCR array data analysis software (http://pcrdataanalysis.sabiosciences.com/pcr/arrayanalysis.php). Total protein was isolated from either whole or cartilaginous portions of limbs from wild type and Runx2 mutant mice. Tissue was flash frozen and pulverized with dounce homogenizer and lysed in 2X SDS lysis buffer. Equal amounts of protein were separated on 10% SDS-polyacrylamide gels. Blots were probed with monoclonal antibody against Runx2 (MBL International, Woburn, MA), Sox9, Sfn and Gpr132 (Santa Cruz Biotechnology, Dallas, TX). Blots were incubated with species matched IRDye-800cw labeled secondary antibodies. Stripped blots were then probed with monoclonal β-tubulin antibody (Sigma-Aldrich, St. Louis, MO). The signals were quantified using Odyssey infrared imaging system (LI-COR Biosciences, Lincoln, NE).

### Chromatin immunoprecipitation, EMSA and immunofluorescence assay

Chromatin immunoprecipitation from chondrogenic cells was performed using ChIP-IT kit (Active Motif, Carlsbad, CA). Briefly, cells were cross linked in 1% formaldehyde/PBS for 10 minutes at 22°C and washed first with PBS and then glycine solution. Cells were collected in PBS containing 5mM PMSF, resuspended in lysis buffer, and sonicated 4 times for 20 seconds each. Gel electrophoresis confirmed that the bulk of DNA fragments from soluble chromatin were ~ 400–500 bp in length. Immunoprecipitation was carried out for 14 hours at 4°C with 5μg of Runx2 M70 antibody (Santa Cruz Biotechnology, Santa Cruz, CA) or normal rabbit IgG as a negative control. The immunoprecipitated chromatin was collected

using Protein A/G beads. Chromatin and 5% input were analyzed by real time PCR using primers designed to amplify promoter fragments spanning the RUNX motif in Sfn, Gpr132, Cyclin A1, and c-Myb genes. The primer sequences and location of RUNX binding sites in each gene are listed in Table S3. In parallel, conventional PCR was performed with 31~37 cycles of amplification. Amplicons were run on a 2% agarose gel, stained with ethidium bromide, and visualized under UV light. The cellular distribution of Runx2 protein and its interaction of Runx2 protein with target DNA were assessed by immunofluorescence and EMSA as described in supplement methods.

### Cloning of promoter-reporter genes and luciferase assay

The Sfn and Gpr132 gene promoter encompassing RUNX motifs were PCR-amplified from C57BL/6 mouse genomic DNA. The forward and reverse primers contained engineered AseI and AgeI restriction sites, respectively (Table S1). The PCR products digested with AseI/AgeI enzymes were ligated into similarly digested EGFP-Luc dual reporter vector. The integrity of both promoters was confirmed with direct sequencing. The GH329 and C3H10T1/2 cells were seeded in twelve-well dishes at a density of $1.5\times10^5$ cells per well and transfected 16 hours later. Cells were co-transfected with Sfn, Gpr132 EGFP-Luc plasmids and varying concentrations of full length or Runx2 Δ369 expression plasmids. The Col Xa and FGF3-Luc vectors were co-transfected with either WT or Δ369 Runx2 expression plasmids and renilla luciferase as an internal control. Luciferase activity was determined 24 hrs later using Luciferase Reporter Assay system (Promega, Madison, WI).

### Cell culture and transient transfections

GH239 cells were cultured in DMEM supplemented with 10% FBS, 4.5g/L glucose, 50 U/ml penicillin G, and 50 mg/ml streptomycin. C3H10T1/2 cells were maintained in MEM supplemented with 10% FBS, 2mM L-glutamine, 50 U/ml penicillin G, and 50 mg/ml streptomycin. For ChIP assays, C3H10T1/2 cells were cultured in a micromass. Briefly, $2\times10^7$ cells were suspended in 1ml medium and 10 μl drops of cell suspension were placed in culture dishes. After 2.5 hours, cells were fed and maintained in chondrogenic media (50ng/ml Ascorbic-acid, 10mM BGPO4, 100ng/ml BMP-2) for 4 days. All transient transfections were performed for 24 hours using PolyJet™ transfection reagent (SignaGen Laboratories Rockville, MD) as per manufacture's instruction.

## Results

### Generation of targeted ES cells and establishment of a Runx2 floxed colony with normal growth and skeletal parameters

To study the spatio-temporal contribution by Runx2 during skeletogenesis, we established a Runx2 floxed model. A targeting vector was constructed by sequential addition of various genomic fragments from the Runx2 locus encompassing intron 7 through the untranslated region of exon 8 (Fig 1 & S1). The presence of LoxP sequences in intron 8 and exon 8 can potentially influence the transcription, stability, or translation of Runx2 mRNA. Thus, we isolated RNA from bone tissues of WT and floxed mice and compared expression levels of Runx2. We used primers in exon 6–7 or exon 8 transcribed regions to confirm the integrity of Runx2 mRNA (Fig S2B). Both primer pairs showed similar levels of expression,

indicating that insertion of LoxP sequences does not modify expression or stability of Runx2 mRNA. Homogenized limbs were used for western blot analysis and, consistent with mRNA expression, all mice showed similar levels of Runx2 protein (Fig S2C). We then monitored the growth of littermates over 80 days. All mice showed a similar but progressive increase in body weight and size over time (Fig S2D). We also compared the overall skeletal growth in these animals at one and four week of age and noted comparable skeletogenesis and mineralization (Fig S2E, F). Thus, our Runx2 exon 8 floxed animals are virtually indistinguishable from normal WT mice. Taken together, these data are reassuring that by themselves, LoxP sequences are not contributing to any phenotype and demonstrate that the activity of the WT Runx2 locus is identical to that of the floxed locus.

### Runx2 functions in chondrocyte are obligatory for endochondral ossification and survival

To elucidate Runx2 regulatory control distinctive to chondrocyte cell population, we used the Col IIa-Cre line (Fig 2, S3). Efficient deletion of Runx2 by Col IIa-Cre recombinase was confirmed with a specific primer pair that simultaneously amplifies both the WT and floxed alleles (Fig 2A). The homozygous mice ($Runx2^{\Delta E8/\Delta E8}$) died shortly after birth and exhibited uniform dwarfism in both axial and appendicular skeleton. Mutant mice were characterized by domed skull, short snout, and small limbs that were often bent inward (Fig 2B). No gross abnormalities of the skeleton were apparent in the $Runx2^{+/\Delta E8}$ mice. Homozygous mutants were recovered with the expected Mendelian frequency, but were significantly lower in weight (Fig 2B, C). Compared with well calcified skeletons in WT and $Runx2^{+/\Delta E8}$ littermates, only a weak alizarin red staining was observed in limbs and pinpoint staining in the dorsal arch of vertebrae and the dorsal part of ribs of newborn mutants (Fig 2D). Many defects ranging from reduced size to irregular shape, angle, and spacing were observed in the axial skeleton of the $Runx2^{\Delta E8/\Delta E8}$ mice. Detailed comparison of the forelimb of homozygous mutants revealed that the scapula was totally cartilaginous and the humerus was extremely small (Fig 2D, E). The radius and ulna were separated but were greatly reduced. Calcification of metacarpals and digits was completely absent in $Runx2^{\Delta E8/\Delta E8}$ mice. Similar developmental failure and abnormalities were noted in the skeletal elements of the hindlimbs of the mutant mice (Fig 2D, E). We noted a poor calcification of dorsal edges of cervical, thoracic, and spine vertebrae, but calcification of centrum, neural spine, caudal vertebrae, pubic, ilium, iliac crests, ischium, and sacrum was completely absent in the $Runx2^{\Delta E8/\Delta E8}$ mice (Fig 2F). The sternum and xiphoid process were completely cartilaginous, where as they were well ossified in both WT and heterozygous littermates (Fig 2F). Since the Col IIa-Cre starts expressing during embryonic development, we assessed endochondral ossification at E16 and E18 (Fig 2G). Calcification of skeletal elements formed by endochondral ossification was noted in WT at E16, but was completely absent in the $Runx2^{\Delta E8/\Delta E8}$ mice. A similar failure of endochondral ossification in mutant mice was evident at E18. We confirmed the Col IIa-Cre activity in the cartilage and chondrocytes with reporter mice (Fig S3). Finally, we established that the endochondral phenotype is due to loss of exon 8 of Runx2 in chondrocytes by western blot analysis (Fig 2H). Total protein isolated from limbs of new born mice showed full length Runx2 protein in wild type mice, while heterozygous showed both full length and Runx2 mutant proteins (Δ369). Homozygous mice showed only the mutant protein. Taken together, our data

demonstrate that exon 8 of Runx2 is indispensable for mouse embryonic development and endochondral ossification.

### Runx2 deficiency results in failed cartilage growth and chondrocyte differentiation

To better understand the cellular phenotype, we carried out histological analysis. The growth plate of WT femurs showed progression into different zones of chondrocytes that change over to calcified cartilage with cortical bone, marrow cavities, and a well expanded ossified zone (Fig 3A). Higher magnification views show chondrocytes with well-defined lacunar rim in WT (Fig 3B, S4). These characteristic features of cartilage and cellular morphology were absent in homozygous femurs (Fig 3A, B, S4). Chondrocyte proliferation and matrix deposition, which is necessary for the interstitial growth process of cartilage, was perturbed in Runx2$^{\Delta E8/\Delta E8}$ mice (Fig 3B, S4). Chondrocyte hypertrophy is a mandatory process during endochondral bone formation. Only few relatively large cells, which barely express type X collagen, could be seen in homozygous femurs (Fig 3C). Overall, the resting zone was greatly expanded and the identifiable proliferating and hypertrophic zones were significantly reduced in the Runx2$^{\Delta E8/\Delta E8}$ growth plate (Fig 3B, D). In WT mice, the extracellular matrix surrounding hypertrophic chondrocytes was permissive to vascular invasion with well-defined ingression of the skeletal cells of the osteoblast lineage and showed presence of RBC and marrow cavities (Fig 3A, S4). However, we did not observe bone marrow in the diaphyseal region of the Runx2$^{\Delta E8/\Delta E8}$ limbs (Fig 3A, S4A). The poor vascularization was further confirmed by immunostaining of CD31, a marker of endothelial cells. In mutant mice, CD31 positive cells were noted at the edges of bone collar and abundantly in the surrounding skeletal muscles (Fig S5A). Unlike WT littermates, the CD31 signal was barely detected in the center of mutant femurs. Thus, the vascular in-growth, which is necessary for marrow cavity formation, does not progress in mutant mice. As a result, the mineralization in the femur of homozygous mice was restricted to bone collars and calcified cartilage (Fig S4B). Taken together, our results demonstrate that Runx2 exon 8 deficiency disrupts growth plate architecture, hypertrophic maturation of chondrocyte, vascular invasion and skeletal development.

### Functional development of chondrocyte and cartilage remodeling is blocked in the absence of Runx2 signaling

Sox9 is a well-documented regulator of cartilage development in the growth plate. To our surprise, the level of Sox9 mRNA in Runx2 $^{\Delta E8/\Delta E8}$ mice was comparable to WT littermates (Fig 4A). Consistent with this observation, similar levels of Sox9 protein was detected in WT and mutant limbs (Fig 4A). Furthermore, similar nuclear distribution of Sox9 protein was noted in WT and mutant growth plate chondrocytes (Fig 4A). These data suggest that the presence of Sox9 alone in chondrocytes is insufficient for regulating later stages of chondrocyte development.

For a molecular understanding of impaired chondrogenesis in Runx2$^{\Delta E8/\Delta E8}$ mice, we analyzed the mRNA of several key signaling molecules and matrix proteins in chondrocytes (Fig 4B). Ihh is expressed in the prehypertrophic chondrocytes and regulates their terminal maturation. We find a significant reduction in levels (2–4 fold) of Ihh mRNA in Runx2$^{\Delta E8/\Delta E8}$ mice. These results are consistent with the near absence of prehypertrophic

and hypertrophic chondrocytes in Runx2 mutant mice. Interestingly, PTHrP expression was normal in Runx2 mutant mice (Fig 4B). This is in sharp contrast to the absence of PTHrP expression noted in Runx2 global null mice. The low level of Ihh did not affect expression of PTHrP, suggesting molecules other than Ihh and Runx2 are involved in the regulation of PTHrP in chondrocytes. Expression of Col Xa was nearly absent in mutant mice, further confirming in situ observation (Fig 3C). In contrast, we observed similar expression levels of Col IIa (Fig 4B). This is consistent with the developmental stage of chondrocytes at which Runx2 is being deleted by Col IIa-Cre recombinase.

Cartilage remodeling by chondroclasts is an integral component of endochondral ossification and vascular invasion in developing bones. The hypertrophic chondrocytes play an essential role in this process through synthesis of VEGF, MMP13, and RANKL. Normal cartilage remodeling was evident with a robust TRAP staining in developing bones of the WT mice (Fig 4C). However, TRAP staining was nearly absent in all skeletal elements of mutant mice. Moreover, VEGF and MMP13 were barely detected in Runx2 mutant chondrocytes (data not shown). This observation is consistent with extremely poor vascularization of $Runx2^{\Delta E8/\Delta E8}$ bones (Fig S4, 5). Near lack of TRAP activity prompted us to determine expression of OPG and RANKL. Expression of both genes was low in mutant mice with a 30% decrease in OPG and 60–80% decrease in RANKL (Fig 4D). This differential expression results in an altered OPG/RANKL ratio that would normally favor inhibition of chondroclast development and cartilage remodeling. Together, our results demonstrate that Runx2 is involved in development of both chondrocyte and chondroclast.

## Nuclear import and DNA binding functions of Runx2 are insufficient for chondrocyte differentiation

The failed endochondral ossification phenotype in $Runx2^{\Delta E8/\Delta E8}$ mice is remarkably similar to the global Runx2 null models. Only the exon 8 encoded portion of the Runx2 protein is deleted in our model; therefore, we assessed functional activities of the mutant Runx2 Δ369 protein (Fig 5). Runx2 is a multipartite transcription factor. The DNA binding region resides in the N-terminus and transcription activation/suppression domain in the C-terminus of the protein (Fig 5A). Western blot analysis of transfected cells shows comparable expression of full length and Δ369 proteins (Fig 5B). This is consistent with similar expression levels of endogenous Runx2 proteins produced in cartilage of WT and mutant mice (Fig 2H). Both proteins exhibited similar cellular distribution and a punctate nuclear pattern that was excluded from nucleoli (Fig 5C). Chondrocytes harvested from the ribs of WT and $Runx2^{\Delta E8/\Delta E8}$ mice at E18.5 also showed presence of Runx2 proteins in nuclear fraction (data not shown). Thus, the skeletal phenotype in homozygous mice is not associated with any changes in expression levels or cellular distribution of Runx2 protein.

To understand if failed development of chondrocyte is linked to altered capacity of Runx2 Δ369 protein to bind target DNA, we performed EMSA. Full length and Runx2 Δ369 protein were transiently expressed in GH329 cells that lack endogenous Runx proteins (Fig 5D). We examined Runx2 protein-DNA interaction with similar sequences of the Runx motifs in the Col Xa, FGF3 and OC promoter. Each of these Runx motifs forms a major complex that is abolished upon mutation of the core sequences (Fig 5D and data not shown).

This complex is not formed on Runx motifs using nuclear extracts from control cells. Interaction of both proteins with DNA was further confirmed by antibody supershift. Interestingly, Runx2 Δ369 loses its interaction with TGFβ-transducer SMAD3, but retains the ability to heterodimerize with Cbfβ partner protein (data not shown). We also assessed transcriptional activity of the WT and Runx2 Δ369 proteins on promoters of FGF3 and Col Xa, a hallmark gene of hypertrophic chondrocytes (Fig 5E). The mutant protein exhibits significantly reduced transactivation of both promoters (Fig 5E). Thus, deletion of exon 8 significantly impairs transcriptional activity of Runx2.

## Runx2 regulates cell cycle genes to control chondrocyte proliferation and cartilage growth

$Runx2^{\Delta E8/\Delta E8}$ mice were dwarfed, indicating lack of both interstitial and appositional growth of cartilage (Fig 2B, 3A). Direct cell count in the resting, proliferating and prehypertrophic regions revealed a dramatic decrease in the total number of cells present in the hyaline cartilage of $Runx2^{\Delta E8/\Delta E8}$ mice (Fig 2, 3). In each region, the total numbers of chondrocytes were roughly half of the wild type (Fig 6A). These differences were not due to increased apoptosis, as cleaved-Caspase 3 staining was similar between WT and mutant chondrocytes (Fig S5B). More importantly, columns of flattened cells, a hallmark of proliferative chondrocytes, were missing in mutant cartilage (Fig 6A). Runx2 role in chondrocyte proliferation *in vivo* was confirmed by BrdU labeling. Runx2 null cartilage showed 45% fewer BrdU positive cells, reflecting a decrease in proliferative capacity of chondrocyte (Fig 6B). Thus, Runx2 is required for chondrocyte proliferation and cartilage growth.

To understand molecular circuitry engaged by Runx2 for chondrocyte proliferation, we determined the expression of genes associated with the cell cycle cascade in the growth plate (Fig 6C). A scatter plot of normalized data with a minimum threshold of 2-fold initially revealed 12 differentially regulated genes in mutant mice. However, mRNA analysis from 3 independent littermates identified 5 genes that consistently showed differential expression. These include membrane receptor (Gpr132), transcription factor (c-Myb), G1/S-G2/M phase cyclins (cyclin A1, A2) and Sfn, a chaperone for signaling transduction (Fig 6C). We next confirmed changes in mRNA levels of these genes by isolating primary chondrocytes from growth plates of an independent litter. The q-PCR reproducibly verified the microarray profile with the exception of cyclin A2 gene (Fig 6D). Runx2 null chondrocytes showed 3 fold higher expression of Sfn mRNA compared to WT cells. Interestingly, a robust suppression ranging from 3–8 fold was consistently noted for Gpr132, c-Myb and cyclin A1 mRNA (Fig 6D). The altered expression of two genes in $Runx2^{\Delta E8/\Delta E8}$ growth plates was also confirmed by western blot analysis (Fig 6E).

To assess if deregulated expression is a consequence of failed chondrocyte development or if these genes are direct targets of Runx2, promoter reporter assays were performed. In silico analysis of 2–3kb genomic sequences upstream of the transcription start site identified multiple high affinity RUNX recognition motifs in all genes. Three RUNX binding sites reside within 1.0 kb of mouse Sfn, cyclin A1, and two in Gpr132 and c-Myb gene promoters (Fig 7A). ChIP data revealed that in chondrocytes, Runx2 protein is bound to these sites (Fig 7B). Occupancy by Runx2 was noted for multiple sites within each gene promoter (Fig 7B).

To assess direct transcriptional regulation, we cloned ~1kb promoter fragment of mouse Gpr132 and Sfn genes in front of EGFP-Luc dual-reporter (Fig 7C, D). Runx2 induced activity of both promoters in a dose-dependent manner. We also compared the transcriptional response of these promoters with Runx2 Δ369 protein, which is expressed in $Runx2^{\Delta E8/\Delta E8}$ mice. The mutant Runx2 protein failed to induce both promoters (Fig 7C, D). The lack of gene promoter response to mutant Runx2 protein is consistent with the chondrocyte phenotype of the mice. Thus through several line of evidence, we have identified a unique set of cell cycle genes that are specifically regulated by Runx2 in chondrocytes.

In summary, exon 8 encoded portion of the Runx2 protein is obligatory for chondrocyte proliferation, hypertrophic maturation, endochondral ossification and survival.

## Discussion

Skeletogenesis in mammals requires coordinated activities of chondrocytes, osteoblasts and osteoclasts. Global Runx2 null mice lack bone tissue formation due to maturational arrest of both chondrocytes and osteoblasts. Here, we report function of endogenous Runx2 in chondrocyte during skeletal development using a novel mouse model. $Runx2^{\Delta E8/\Delta E8}$ mice exhibited disrupted chondrocyte development and failed endochondral ossification. We demonstrate that nuclear import or DNA binding activities of Runx2 are not sufficient for chondrocyte differentiation and endochondral ossification. Skeletal elements formed by endochondral process are devoid of hypertrophic chondrocytes, vasculature, and marrow. Molecular studies reveal that disruption of chondrocyte differentiation in Runx2 mutant mice is independent of PTHrP and Sox9 expression. Runx2 function in chondrocytes also regulates OPG-RANKL signaling required for cartilage resorption. Surprisingly, Runx2 deficiency perturbs chondrocyte proliferation through regulating a unique set of cell cycle genes.

Runx2 is a modular transcription factor. Nuclear import, sequence specific DNA binding, interaction with heteromeric partner Cbfβ, and a part of the transcription activation domain reside within the N-terminus. The C-terminus contains a context dependent transcription activation/suppression domain, the nuclear matrix targeting signal, and regions for physical interactions with transducer proteins of various signaling pathways (19,31–33). We deleted exon 8 of the Runx2 gene that encodes one-third of the Runx2 protein and most of the C-terminus. We show Runx2 Δ369 protein is present in the nucleus, binds target DNA, maintains protein interaction in the N-terminus, but exhibits very low transcriptional activity. At this point, we do not know the resident time of Runx2 Δ369 protein at the target gene promoter and if it is linked with reduced transcriptional activity. In other models, the N-terminal RHD encoded by exon 2–4 of Runx2 gene has been targeted (21,28,34). The RHD targeting will result either in the loss of DNA binding and interaction with Cbfβ, or in blockage of nuclear import of Runx2 protein. Most likely, Runx2 protein is unstable in these models, as nuclear import and Cbfβ interaction are important for Runx2 protein stability. However, our studies identify that the C-terminal region encoded by exon 8 drives critical biological activity of the Runx2 protein. This region is obligatory for both chondrocyte proliferation and differentiation during endochondral ossification.

Endochondral ossification is a sequential process that involves chondrocyte proliferation, differentiation, cartilage calcification, cell death, resorption, and eventual remodeling into bone tissue. Runx2 has largely been associated with chondrocyte hypertrophy and osteoblast commitment. The lack of chondrocyte hypertrophy in our mice is consistent with global null and knock-in models of Runx2 (19,21). However, our studies identify that a major function of Runx2 in cartilage is to regulate chondrocyte proliferation. Direct cell count and in vivo BrdU labeling demonstrate that Runx2 promotes the proliferative capacity of chondrocytes. The limbs of $Runx2^{\Delta E8/\Delta E8}$ mice are ~20% smaller than wild type at E18 and 35% smaller at new born stage. This difference in growth is primarily attributed to a 50% decrease in chondrocyte proliferation. Our data is consistent with the decrease in chondrocyte proliferation reported in global Runx2 null mice and the expression of Runx2 in proliferating chondrocytes (16,25,35–37). Interestingly, Runx2 mediated regulation of chondrocyte proliferation is also found in permanent cartilage. It is important to note that Runx2 inhibits the proliferation of calvarial osteoblasts (38). Thus, Runx2 differentially regulates proliferative capacity of skeletal lineage cells. Runx2 promote proliferation of chondrocyte but actively inhibit proliferation of osteoblast. It is reasonable to assume that Runx2 also regulates proliferative capacity of chondrocytes in postnatal mice and functions in primordial dwarfism, but due to perinatal lethality, we are unable to assess this in the Col IIa-Runx2 null model.

To identify Runx2 target genes involved in chondrocyte proliferation, we performed gene array analysis. Only 5% of the tested cell cycle related genes consistently showed a difference in expression in Runx2 null chondrocytes. The Sfn (14-3-3σ) is significantly upregulated in Runx2 null chondrocytes. This change was confirmed by both RNA and protein analysis. Sfn functions as an intracellular chaperone for signal transduction and cell cycle regulation (39). Sfn induces G2 arrest and prevents initiation of mitosis by cytoplasmic sequestration of the Cdk2/Cdk4 -cyclin B1 complex (40,41). Interestingly, Sfn mutant mice die at birth due to respiratory failure and display severe shortening of limbs, which indicates impaired growth of cartilage (42). Recent reports show Sfn sequesters phosphorylated HDAC4 in the cytoplasm to regulate chondrocyte differentiation in the growth plate (43,44). Thus, decreased chondrocyte proliferation and reduced size of hyaline cartilage in $Runx2^{\Delta E8/\Delta E8}$ mice is consistent with high levels of Sfn, a negative regulator of cell cycle progression.

Expression of Gpr132, c-Myb, cyclin A1and cycline A2 was reduced in Runx2 null chondrocytes. The Gpr132 protein causes cell cycle arrest at the G2/M phase and is activated by oxidative stress and other stimuli (45). Although Gpr132 is a Runx2 target gene, Gpr132 null mice do not show skeletal abnormalities. The transcription factor, c-Myb, is a critical regulator of proliferation and stem cell differentiation (46). c-Myb regulates the cell cycle through interaction with cyclin D1 and Cdk4/Cdk6, and by transcriptional regulation of cyclin B1/cyclin E1 (47). The c-Myb null mice die at the onset of endochondral ossification due to failed erythropoiesis (48). The cyclin A protein functions at both G1/S and G2/M phase transitions (49). Cyclin A1 is expressed in testis, calvarial osteoblasts, embryonic fibroblasts and bone marrow cells. Cyclin A1 deficient mice show no skeletal phenotype, but cyclin A2 null mice die in utero long before the initiation of skeletogenesis (50,51). Interestingly, cyclin A1 reduction in conjuction with c-Myb is

associated with decreased proliferation and maintenance of pluripotency of iPS cells (52). Thus, proliferative defects in Runx2 null chondrocytes reflect combined changes in multiple cell cycle regulatory genes.

To better understand the molecular signaling involved in Runx2 regulated chondrocyte proliferation and differentiation, we performed gene expression analysis. The PTHrP-Ihh signaling regulates chondrogenesis by both enhancing chondrocyte proliferation and inhibiting chondrocyte hypertrophy (5,53). Ihh produced by prehypertrophic chondrocytes activates PTHrP expression in resting chondrocytes to promote chondrocyte proliferation and inhibit chondrocyte hypertrophy. Consistent with an earlier report showing Ihh is a downstream target of Runx2, we noted lower expression level of Ihh in $Runx2^{\Delta E8/\Delta E8}$ null chondrocytes (25). PTHrP is not expressed in global Runx2 null mice (24). Surprisingly, normal levels of PTHrP were noted in Runx2 null chondrocytes, indicating that a full dosage of Ihh is not required for PTHrP expression in chondrocytes. PTHrP has been shown to maintain chondrocyte proliferation and delay hypertrophy by phosphorylating Sox9 (54). However, recent reports indicate that Sox9 also plays a role in promoting chondrocyte hypertrophy (16). Haploinsufficiency of Sox9 in chondrocytes results in severe chondrodysplasia and lethality at birth. Interestingly, Runx2 is absent in the limbs of these mice (15). In our model, WT and mutant chondrocytes show similar level of Sox9 mRNA and protein. Thus, inhibition of chondrocyte proliferation in our model is surprising, especially with normal levels of both PTHrP and Sox9. Although detailed mechanism remains to be investigated, these results suggest Sox9 mediated regulation of chondrocyte proliferative capacity and hypertrophy requires obligatory presence of Runx2. In this regard, physical and functional interaction between Runx2 and Sox9 are documented at the Col Xa promoter (55). Thus, it is likely that upon commitment of mesenchymal precursors to the chondrogenic lineage, both Sox9 and Runx2 are necessary for progression of chondrogenesis.

Remodeling of cartilage is the last critical step for endochondral ossification. We observed multinucleated TRAP-positive cells, either osteoclasts or chondroclasts in the wild type animals but not in the $Runx2^{\Delta E8/\Delta E8}$ mice. Development of functional chondroclasts from the monocyte lineage requires RANKL produced by various mesenchymal and endothelial cells (56). Since hyaline cartilage is an avascular tissue, local expression of RANKL by chondrocytes plays a major role for chondroclast development (57,58). Hypertrophic chondrocytes are the main source of cartilaginous RANKL (56,58). Deletion of Runx2 in chondrocytes causes a dramatic reduction in RANKL and a modest decrease in OPG expression. The resultant change in ratio of OPG/RANKL in Runx2 mutants leads to inhibition of chondroclast development. It is unlikely that lack of hypertrophic chondrocytes alone is the reason for the loss of RANKL expression in limbs of mutant mice. Runx2 is known to regulate RANKL gene expression in chondrocytes (59). Thus, Runx2 also plays a role in chondroclast maturation and the process of cartilage resorption. Taken together, our observations establish novel functions of Runx2 that extend beyond the differentiation process of chondrocytes.

## Supplementary Material

Refer to Web version on PubMed Central for supplementary material.

## Acknowledgments

This work was supported by Grant No. R01AG030228, R01AR062091 from the National Institutes of Health.

## References

1. Karsenty G, Kronenberg HM, Settembre C. Genetic control of bone formation. Annu Rev Cell Dev Biol. 2009; 25:629–48. [PubMed: 19575648]
2. Lefebvre V, Smits P. Transcriptional control of chondrocyte fate and differentiation. Birth Defects Res C Embryo Today. 2005; 75(3):200–12. [PubMed: 16187326]
3. Minina E, Wenzel HM, Kreschel C, Karp S, Gaffield W, McMahon AP, Vortkamp A. BMP and Ihh/PTHrP signaling interact to coordinate chondrocyte proliferation and differentiation. Development. 2001; 128(22):4523–34. [PubMed: 11714677]
4. Kronenberg HM. PTHrP and skeletal development. Ann N Y Acad Sci. 2006; 1068:1–13. [PubMed: 16831900]
5. St-Jacques B, Hammerschmidt M, McMahon AP. Indian hedgehog signaling regulates proliferation and differentiation of chondrocytes and is essential for bone formation. Genes Dev. 1999; 13(16): 2072–86. [PubMed: 10465785]
6. Guo J, Chung UI, Yang D, Karsenty G, Bringhurst FR, Kronenberg HM. PTH/PTHrP receptor delays chondrocyte hypertrophy via both Runx2-dependent and -independent pathways. Dev Biol. 2006; 292(1):116–28. [PubMed: 16476422]
7. Vortkamp A, Lee K, Lanske B, Segre GV, Kronenberg HM, Tabin CJ. Regulation of rate of cartilage differentiation by Indian hedgehog and PTH-related protein. Science. 1996; 273(5275): 613–22. [PubMed: 8662546]
8. Karaplis AC, Luz A, Glowacki J, Bronson RT, Tybulewicz VL, Kronenberg HM, Mulligan RC. Lethal skeletal dysplasia from targeted disruption of the parathyroid hormone-related peptide gene. Genes Dev. 1994; 8(3):277–89. [PubMed: 8314082]
9. Amizuka N, Warshawsky H, Henderson JE, Goltzman D, Karaplis AC. Parathyroid hormone-related peptide-depleted mice show abnormal epiphyseal cartilage development and altered endochondral bone formation. J Cell Biol. 1994; 126(6):1611–23. [PubMed: 8089190]
10. Karp SJ, Schipani E, St-Jacques B, Hunzelman J, Kronenberg H, McMahon AP. Indian hedgehog coordinates endochondral bone growth and morphogenesis via parathyroid hormone related-protein-dependent and -independent pathways. Development. 2000; 127(3):543–8. [PubMed: 10631175]
11. Minina E, Kreschel C, Naski MC, Ornitz DM, Vortkamp A. Interaction of FGF, Ihh/Pthlh, and BMP signaling integrates chondrocyte proliferation and hypertrophic differentiation. Dev Cell. 2002; 3(3):439–49. [PubMed: 12361605]
12. Zou H, Niswander L. Requirement for BMP signaling in interdigital apoptosis and scale formation. Science. 1996; 272(5262):738–41. [PubMed: 8614838]
13. Zou H, Wieser R, Massague J, Niswander L. Distinct roles of type I bone morphogenetic protein receptors in the formation and differentiation of cartilage. Genes Dev. 1997; 11(17):2191–203. [PubMed: 9303535]
14. Spater D, Hill TP, O'Sullivan RJ, Gruber M, Conner DA, Hartmann C. Wnt9a signaling is required for joint integrity and regulation of Ihh during chondrogenesis. Development. 2006; 133(15): 3039–49. [PubMed: 16818445]
15. Akiyama H, Chaboissier MC, Martin JF, Schedl A, de Crombrugghe B. The transcription factor Sox9 has essential roles in successive steps of the chondrocyte differentiation pathway and is required for expression of Sox5 and Sox6. Genes Dev. 2002; 16(21):2813–28. [PubMed: 12414734]

16. Dy P, Wang W, Bhattaram P, Wang Q, Wang L, Ballock RT, Lefebvre V. Sox9 directs hypertrophic maturation and blocks osteoblast differentiation of growth plate chondrocytes. Dev Cell. 2012; 22(3):597–609. [PubMed: 22421045]
17. Bell DM, Leung KK, Wheatley SC, Ng LJ, Zhou S, Ling KW, Sham MH, Koopman P, Tam PP, Cheah KS. SOX9 directly regulates the type-II collagen gene. Nat Genet. 1997; 16(2):174–8. [PubMed: 9171829]
18. Smits P, Li P, Mandel J, Zhang Z, Deng JM, Behringer RR, de Crombrugghe B, Lefebvre V. The transcription factors L-Sox5 and Sox6 are essential for cartilage formation. Dev Cell. 2001; 1(2): 277–90. [PubMed: 11702786]
19. Choi JY, Pratap J, Javed A, Zaidi SK, Xing L, Balint E, Dalamangas S, Boyce B, van Wijnen AJ, Lian JB, Stein JL, Jones SN, Stein GS. Subnuclear targeting of Runx/Cbfa/AML factors is essential for tissue-specific differentiation during embryonic development. Proc Natl Acad Sci U S A. 2001; 98(15):8650–5. [PubMed: 11438701]
20. Hinoi E, Bialek P, Chen YT, Rached MT, Groner Y, Behringer RR, Ornitz DM, Karsenty G. Runx2 inhibits chondrocyte proliferation and hypertrophy through its expression in the perichondrium. Genes Dev. 2006; 20(21):2937–42. [PubMed: 17050674]
21. Komori T, Yagi H, Nomura S, Yamaguchi A, Sasaki K, Deguchi K, Shimizu Y, Bronson RT, Gao YH, Inada M, Sato M, Okamoto R, Kitamura Y, Yoshiki S, Kishimoto T. Targeted disruption of Cbfa1 results in a complete lack of bone formation owing to maturational arrest of osteoblasts. Cell. 1997; 89(5):755–64. [PubMed: 9182763]
22. Takeda S, Bonnamy JP, Owen MJ, Ducy P, Karsenty G. Continuous expression of Cbfa1 in nonhypertrophic chondrocytes uncovers its ability to induce hypertrophic chondrocyte differentiation and partially rescues Cbfa1-deficient mice. Genes Dev. 2001; 15(4):467–81. [PubMed: 11230154]
23. Ueta C, Iwamoto M, Kanatani N, Yoshida C, Liu Y, Enomoto-Iwamoto M, Ohmori T, Enomoto H, Nakata K, Takada K, Kurisu K, Komori T. Skeletal malformations caused by overexpression of Cbfa1 or its dominant negative form in chondrocytes. J Cell Biol. 2001; 153(1):87–100. [PubMed: 11285276]
24. Inada M, Yasui T, Nomura S, Miyake S, Deguchi K, Himeno M, Sato M, Yamagiwa H, Kimura T, Yasui N, Ochi T, Endo N, Kitamura Y, Kishimoto T, Komori T. Maturational disturbance of chondrocytes in Cbfa1-deficient mice. Dev Dyn. 1999; 214(4):279–90. [PubMed: 10213384]
25. Yoshida CA, Yamamoto H, Fujita T, Furuichi T, Ito K, Inoue K, Yamana K, Zanma A, Takada K, Ito Y, Komori T. Runx2 and Runx3 are essential for chondrocyte maturation, and Runx2 regulates limb growth through induction of Indian hedgehog. Genes Dev. 2004; 18(8):952–63. [PubMed: 15107406]
26. Ding M, Lu Y, Abbassi S, Li F, Li X, Song Y, Geoffroy V, Im HJ, Zheng Q. Targeting Runx2 expression in hypertrophic chondrocytes impairs endochondral ossification during early skeletal development. J Cell Physiol. 2012; 227(10):3446–56. [PubMed: 22223437]
27. Chen H, Ghori-Javed FY, Rashid H, Serra R, Gutierrez SE, Javed A. Chondrocyte-specific regulatory activity of Runx2 is essential for survival and skeletal development. Cells Tissues Organs. 2011; 194(2–4):161–5. [PubMed: 21597273]
28. Takarada T, Hinoi E, Nakazato R, Ochi H, Xu C, Tsuchikane A, Takeda S, Karsenty G, Abe T, Kiyonari H, Yoneda Y. An analysis of skeletal development in osteoblast-specific and chondrocyte-specific runt-related transcription factor-2 (Runx2) knockout mice. J Bone Miner Res. 2013; 28(10):2064–9. [PubMed: 23553905]
29. Ovchinnikov DA, Deng JM, Ogunrinu G, Behringer RR. Col2a1-directed expression of Cre recombinase in differentiating chondrocytes in transgenic mice. Genesis. 2000; 26(2):145–6. [PubMed: 10686612]
30. Soriano P. Generalized lacZ expression with the ROSA26 Cre reporter strain. Nat Genet. 1999; 21(1):70–1. [PubMed: 9916792]
31. Lian JB, Javed A, Zaidi SK, Lengner C, Montecino M, van Wijnen AJ, Stein JL, Stein GS. Regulatory controls for osteoblast growth and differentiation: role of Runx/Cbfa/AML factors. Crit Rev Eukaryot Gene Expr. 2004; 14(1–2):1–41. [PubMed: 15104525]

32. Javed A, Bae JS, Afzal F, Gutierrez S, Pratap J, Zaidi SK, Lou Y, van Wijnen AJ, Stein JL, Stein GS, Lian JB. Structural coupling of Smad and Runx2 for execution of the BMP2 osteogenic signal. J Biol Chem. 2008; 283(13):8412–22. [PubMed: 18204048]
33. Schroeder TM, Jensen ED, Westendorf JJ. Runx2: a master organizer of gene transcription in developing and maturing osteoblasts. Birth Defects Res C Embryo Today. 2005; 75(3):213–25. [PubMed: 16187316]
34. Otto F, Thornell AP, Crompton T, Denzel A, Gilmour KC, Rosewell IR, Stamp GW, Beddington RS, Mundlos S, Olsen BR, Selby PB, Owen MJ. Cbfa1, a candidate gene for cleidocranial dysplasia syndrome, is essential for osteoblast differentiation and bone development. Cell. 1997; 89(5):765–71. [PubMed: 9182764]
35. Chen D, Bashur LA, Liang B, Panattoni M, Tamai K, Pardi R, Zhou G. The transcriptional co-regulator Jab1 is crucial for chondrocyte differentiation in vivo. J Cell Sci. 2013; 126(Pt 1):234–43. [PubMed: 23203803]
36. Shu B, Zhang M, Xie R, Wang M, Jin H, Hou W, Tang D, Harris SE, Mishina Y, O'Keefe RJ, Hilton MJ, Wang Y, Chen D. BMP2, but not BMP4, is crucial for chondrocyte proliferation and maturation during endochondral bone development. J Cell Sci. 2011; 124(Pt 20):3428–40. [PubMed: 21984813]
37. Tang GH, Rabie AB. Runx2 regulates endochondral ossification in condyle during mandibular advancement. J Dent Res. 2005; 84(2):166–71. [PubMed: 15668335]
38. Pratap J, Galindo M, Zaidi SK, Vradii D, Bhat BM, Robinson JA, Choi JY, Komori T, Stein JL, Lian JB, Stein GS, van Wijnen AJ. Cell growth regulatory role of Runx2 during proliferative expansion of preosteoblasts. Cancer Res. 2003; 63(17):5357–62. [PubMed: 14500368]
39. Hermeking H. The 14-3-3 cancer connection. Nat Rev Cancer. 2003; 3(12):931–43. [PubMed: 14737123]
40. Chan TA, Hermeking H, Lengauer C, Kinzler KW, Vogelstein B. 14-3-3Sigma is required to prevent mitotic catastrophe after DNA damage. Nature. 1999; 401(6753):616–20. [PubMed: 10524633]
41. Laronga C, Yang HY, Neal C, Lee MH. Association of the cyclin-dependent kinases and 14-3-3 sigma negatively regulates cell cycle progression. J Biol Chem. 2000; 275(30):23106–12. [PubMed: 10767298]
42. Herron BJ, Liddell RA, Parker A, Grant S, Kinne J, Fisher JK, Siracusa LD. A mutation in stratifin is responsible for the repeated epilation (Er) phenotype in mice. Nat Genet. 2005; 37(11):1210–2. [PubMed: 16200063]
43. Guan Y, Chen Q, Yang X, Haines P, Pei M, Terek R, Wei X, Zhao T, Wei L. Subcellular relocation of histone deacetylase 4 regulates growth plate chondrocyte differentiation through Ca2+/calmodulin-dependent kinase IV. Am J Physiol Cell Physiol. 2012; 303(1):C33–40. [PubMed: 22442139]
44. Vega RB, Matsuda K, Oh J, Barbosa AC, Yang X, Meadows E, McAnally J, Pomajzl C, Shelton JM, Richardson JA, Karsenty G, Olson EN. Histone deacetylase 4 controls chondrocyte hypertrophy during skeletogenesis. Cell. 2004; 119(4):555–66. [PubMed: 15537544]
45. Weng Z, Fluckiger AC, Nisitani S, Wahl MI, Le LQ, Hunter CA, Fernal AA, Le Beau MM, Witte ON. A DNA damage and stress inducible G protein-coupled receptor blocks cells in G2/M. Proc Natl Acad Sci U S A. 1998; 95(21):12334–9. [PubMed: 9770487]
46. Quintana AM, Zhou YE, Pena JJ, O'Rourke JP, Ness SA. Dramatic repositioning of c-Myb to different promoters during the cell cycle observed by combining cell sorting with chromatin immunoprecipitation. PLoS One. 2011; 6(2):e17362. [PubMed: 21364958]
47. Nakata Y, Shetzline S, Sakashita C, Kalota A, Rallapalli R, Rudnick SI, Zhang Y, Emerson SG, Gewirtz AM. c-Myb contributes to G2/M cell cycle transition in human hematopoietic cells by direct regulation of cyclin B1 expression. Mol Cell Biol. 2007; 27(6):2048–58. [PubMed: 17242210]
48. Mucenski ML, McLain K, Kier AB, Swerdlow SH, Schreiner CM, Miller TA, Pietryga DW, Scott WJ Jr, Potter SS. A functional c-myb gene is required for normal murine fetal hepatic hematopoiesis. Cell. 1991; 65(4):677–89. [PubMed: 1709592]

49. Cardoso MC, Leonhardt H, Nadal-Ginard B. Reversal of terminal differentiation and control of DNA replication: cyclin A and Cdk2 specifically localize at subnuclear sites of DNA replication. Cell. 1993; 74(6):979–92. [PubMed: 8402887]
50. Liu D, Matzuk MM, Sung WK, Guo Q, Wang P, Wolgemuth DJ. Cyclin A1 is required for meiosis in the male mouse. Nat Genet. 1998; 20(4):377–80. [PubMed: 9843212]
51. Murphy M, Stinnakre MG, Senamaud-Beaufort C, Winston NJ, Sweeney C, Kubelka M, Carrington M, Brechot C, Sobczak-Thepot J. Delayed early embryonic lethality following disruption of the murine cyclin A2 gene. Nat Genet. 1997; 15(1):83–6. [PubMed: 8988174]
52. McLenachan S, Menchon C, Raya A, Consiglio A, Edel MJ. Cyclin A1 is essential for setting the pluripotent state and reducing tumorigenicity of induced pluripotent stem cells. Stem Cells Dev. 2012; 21(15):2891–9. [PubMed: 22500553]
53. Provot S, Schipani E. Molecular mechanisms of endochondral bone development. Biochem Biophys Res Commun. 2005; 328(3):658–65. [PubMed: 15694399]
54. Huang W, Chung UI, Kronenberg HM, de Crombrugghe B. The chondrogenic transcription factor Sox9 is a target of signaling by the parathyroid hormone-related peptide in the growth plate of endochondral bones. Proc Natl Acad Sci U S A. 2001; 98(1):160–5. [PubMed: 11120880]
55. Zhou G, Zheng Q, Engin F, Munivez E, Chen Y, Sebald E, Krakow D, Lee B. Dominance of SOX9 function over RUNX2 during skeletogenesis. Proc Natl Acad Sci U S A. 2006; 103(50): 19004–9. [PubMed: 17142326]
56. O'Brien CA. Control of RANKL gene expression. Bone. 2010; 46(4):911–9. [PubMed: 19716455]
57. Dougall WC, Glaccum M, Charrier K, Rohrbach K, Brasel K, De Smedt T, Daro E, Smith J, Tometsko ME, Maliszewski CR, Armstrong A, Shen V, Bain S, Cosman D, Anderson D, Morrissey PJ, Peschon JJ, Schuh J. RANK is essential for osteoclast and lymph node development. Genes Dev. 1999; 13(18):2412–24. [PubMed: 10500098]
58. Xiong J, Onal M, Jilka RL, Weinstein RS, Manolagas SC, O'Brien CA. Matrix-embedded cells control osteoclast formation. Nat Med. 2011; 17(10):1235–41. [PubMed: 21909103]
59. Usui M, Xing L, Drissi H, Zuscik M, O'Keefe R, Chen D, Boyce BF. Murine and chicken chondrocytes regulate osteoclastogenesis by producing RANKL in response to BMP2. J Bone Miner Res. 2008; 23(3):314–25. [PubMed: 17967138]

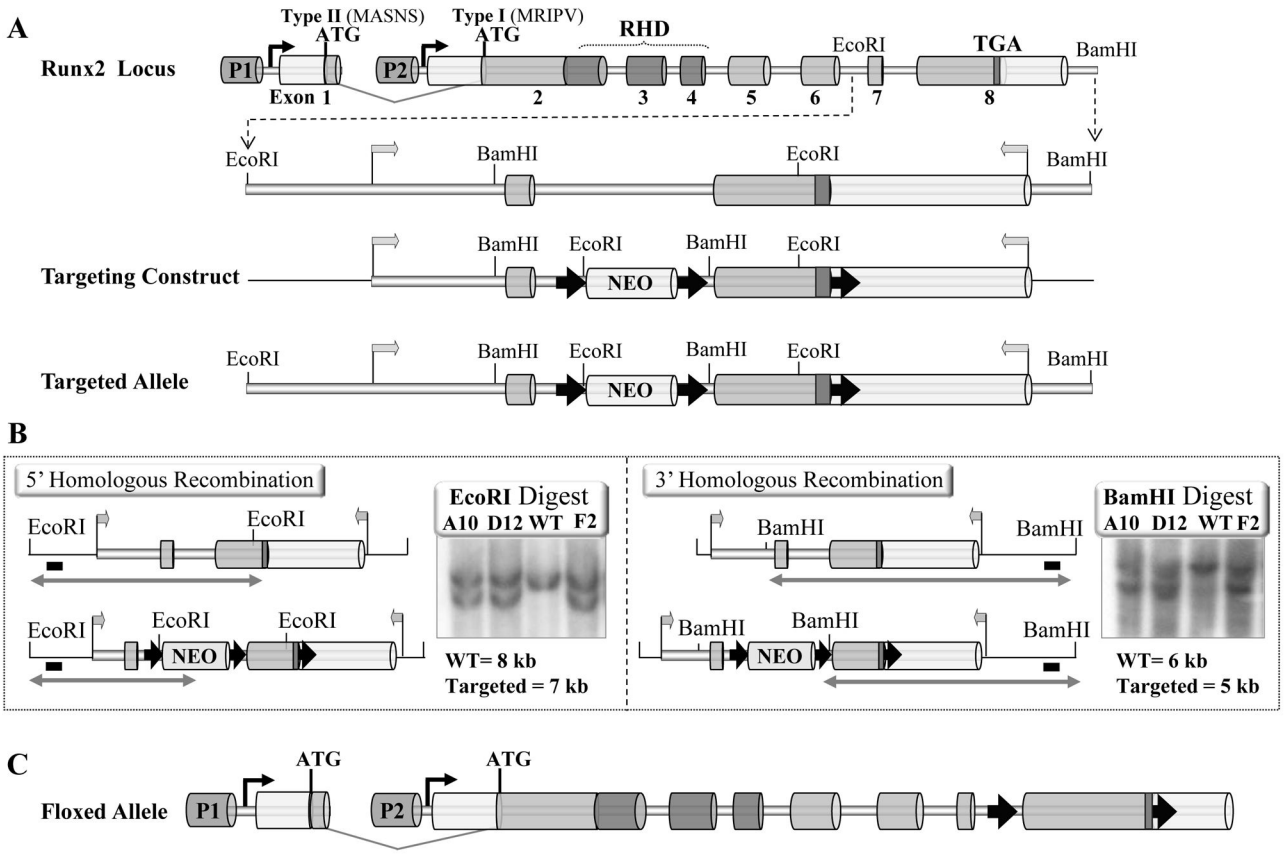


**Figure 1. Genomic organization of Runx2 locus and strategy for generating exon 8 floxed targeting vector**

(**A**) Schematic illustration of exons 1–8 (drawn to scale), that constitute the Runx2 gene and the origin of the type I and type II isoforms from independent promoters. The RHD (exon 2–4, dark grey) and the 5′ and 3′ untranslated regions (light grey) are specified. The genomic region from intron 7 to exon 8 with the key restriction sites used to clone the LoxP site is indicated below. Floxed neomycin gene was cloned 0.9kb upstream of exon 8 and a directional LoxP site (black arrow) was introduced 10bp after stop codon. (B) Southern blot analysis of the primary ES cells with correct homologous recombination confirmed with 5′ and 3′ external genomic probes. The BamHI and EcoRI restriction sites in the endogenous and targeted Runx2 locus are indicated. Double headed arrow indicates the expected size of the Runx2 gene fragment released from respective allele. Thick black line shows the position of probes. A10, D12 and F2 are positive ES cell clones. WT represent control ES cells. (C) Illustration of the genomic Runx2 locus after proper homologous recombination and removal of floxed Neo gene.

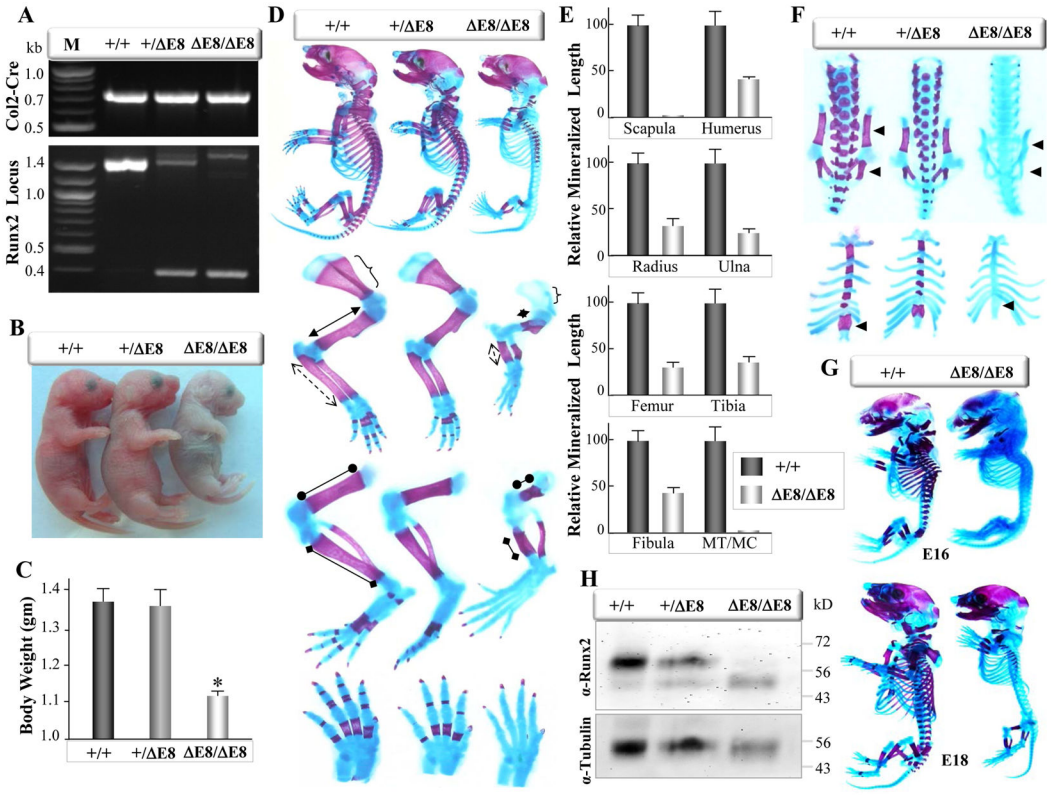


**Figure 2. Runx2 gene deletion in chondrocyte causes lethality and failed endochondral ossification**

(A) PCR confirmation of genotypes from E18 littermates with primer pair that simultaneously amplifies the +/+, +/ΔE8, and ΔE8/ΔE8 Runx2 alleles. (B) Gross appearance of the new born littermates. Homozygous mutants are significantly smaller and die immediately after birth. (C) Pooled data of body weight from 6 mice of each genotype show significant difference ($p<0.05$) in homozygous mice. (D) Assessment of skeletogenesis in the new born pups with alcian blue and alizarin red staining. Scapula (right brace), humerus (double headed arrow), radius and ulna (double headed doted arrow) of WT, heterozygous and Runx2$^{\Delta E8/\Delta E8}$ mice are shown. Mineralizing parts of hind limb bones (tibia and femur) are greatly reduced in Runx2$^{\Delta E8/\Delta E8}$ mice. Metatarsal, metacarpal and digits of the mutant mice completely lack mineralization. (E) The lengths of mineralized portion of various skeletal elements were measured and pooled data from 3 W and 3 mutant mice is presented in the bar graph. (F) Comparison of axial skeleton shows mineralization is completely absent in vertebrae, spine and pubic bones (arrow heads) of homozygous mice. Ossification of the sternum and xiphoid process is totally absent in Runx2$^{\Delta E8/\Delta E8}$ mice. (G) Stained skeletal preparation shows age appropriate arrest in endochondral ossification at E16 and E18. (H) Proteins isolated from limbs of new born littermates were subjected to SDS-PAGE. Blots were probed with Runx2 antibody, striped and reprobed for β-tubulin used as a loading control. Exon 8 truncated Runx2 protein is noted only in the mutant mice.

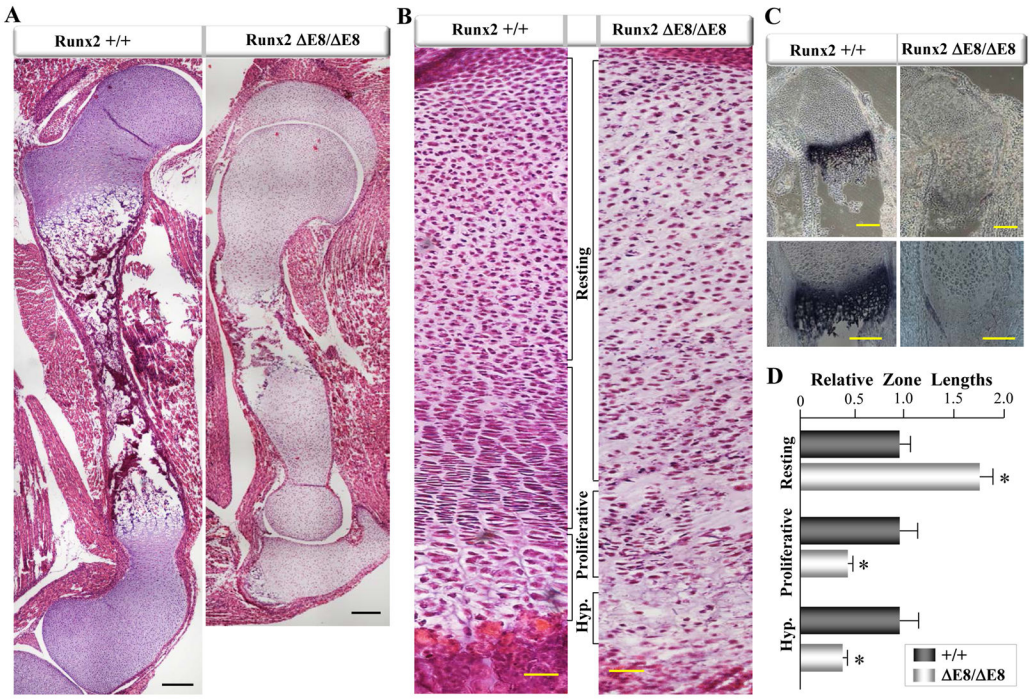


**Figure 3. Failed differentiation of chondrocyte in Runx2$^{\Delta E8/\Delta E8}$ mice**

Limbs from 4 WT and 4 Runx2$^{\Delta E8/\Delta E8}$ new born mice from independent litters were processed for histological analysis. (A) Twenty four individual images captured at 10x magnification were stitched together digitally. A representative image of whole femur stained with hematoxylin and eosin is shown. (B) WT and Runx2$^{\Delta E8/\Delta E8}$ femurs were processed for frozen sections. Epiphysis to calcified region is shown at 40X magnification. Distinct zones of proliferative and hypertrophic chondrocytes were absent in homozygous mice. (C) Representative images of type X collagen in situ hybridization at proximal (upper) and distal (lower) end of growth plate are presented. (D) Five alternate sections covering central part of the WT and homozygous femurs were stained with H&E. Lengths of various zones at the proximal end of growth plate were measured using Nikon NIS-Elements software. In Runx2$^{\Delta E8/\Delta E8}$ femurs, presence of more than two flat chondrocyte in a column was considered as proliferative zone and region between the calcified and stacks of columnar cells as hypertrophic zone. Data from three sections each from 2 WT and 2 mutant mice was pooled and average zone length relative to WT is shown in graph. Scale bars are 200μm.

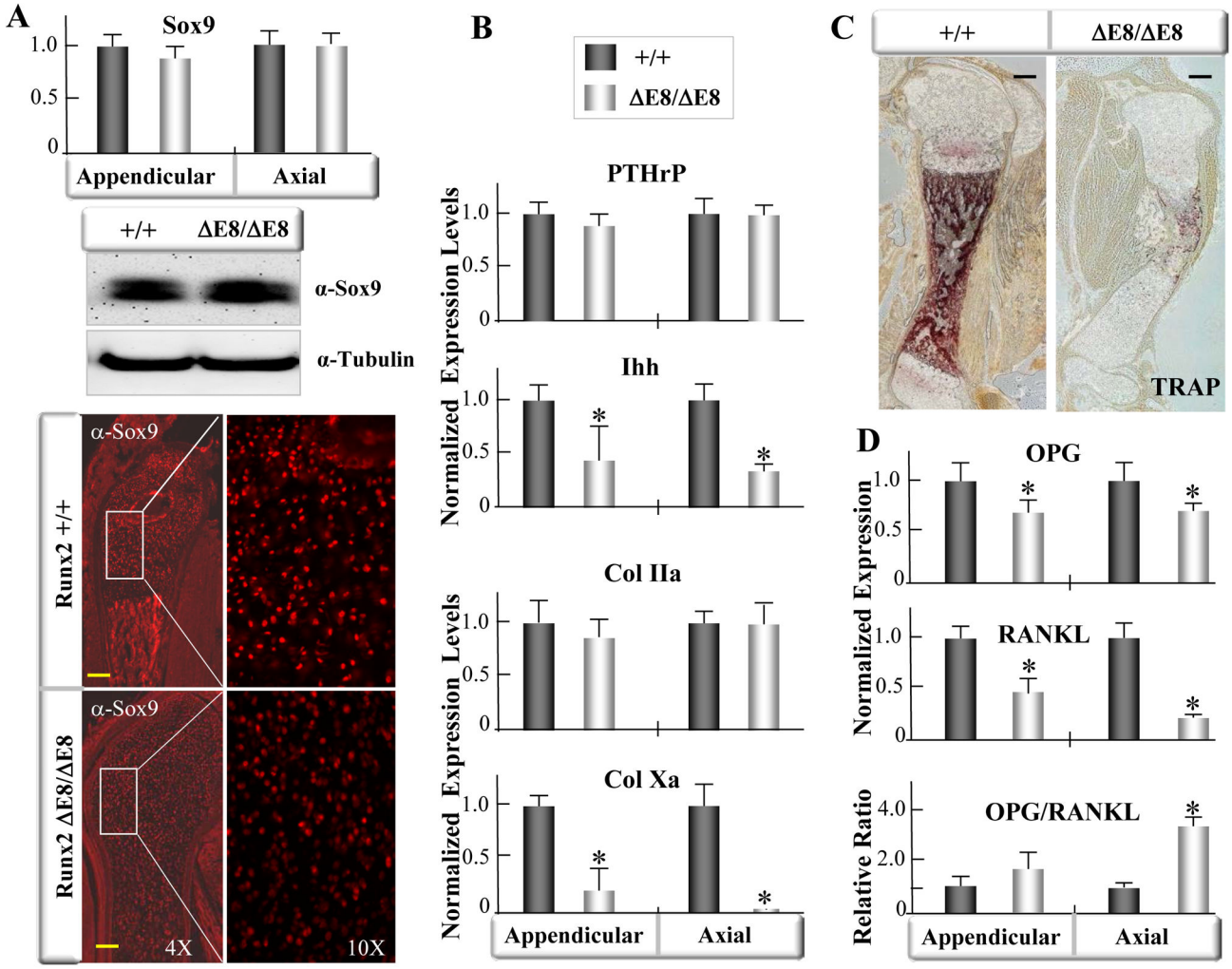


**Figure 4. PTHrP-Ihh regulatory loop and RANKL-OPG signaling are perturbed in Runx2 mutant chondrocytes**

Axial (rib, spine, tail) and appendicular (limbs) skeletal elements from 4 WT and 4 $Runx2^{\Delta E8/\Delta E8}$ embryos at E17.5 were harvested for RNA isolation. The mRNA expression in these samples (n=4) was detected by real-time PCR in triplicates. (A) Similar level of Sox9 mRNA was noted in the WT and $Runx2^{\Delta E8/\Delta E8}$ mice. Limbs from E18.5 embryos were homogenized to isolate protein. Western blot was probed with indicated antibodies. Representative image of Sox9 signals in chondrocyte of E18.5 femur from WT and $Runx2^{\Delta E8/\Delta E8}$ mice are shown at 4X and 10X magnifications (boxed). (B) Levels of PTHrP, Ihh, Col IIa and Col Xa mRNA in axial and appendicular skeletal elements. Data were normalized with beta-actin and are presented as relative to WT. (C) WT and mutant new born femurs were processed for TRAP staining to monitor osteoclast and chondroclast activity. TRAP staining was barely detected in $Runx2^{\Delta E8/\Delta E8}$ mice. (D) Significant decrease was noted in OPG and RANKL mRNA. Ratio of OPG/RANKL was calculated based on the expression levels of respective genes. Asterisks denote significant difference in pooled values from 4 WT and 4 $Runx2^{\Delta E8/\Delta E8}$ embryos ($p<0.05$). Scale bars are 200μm.

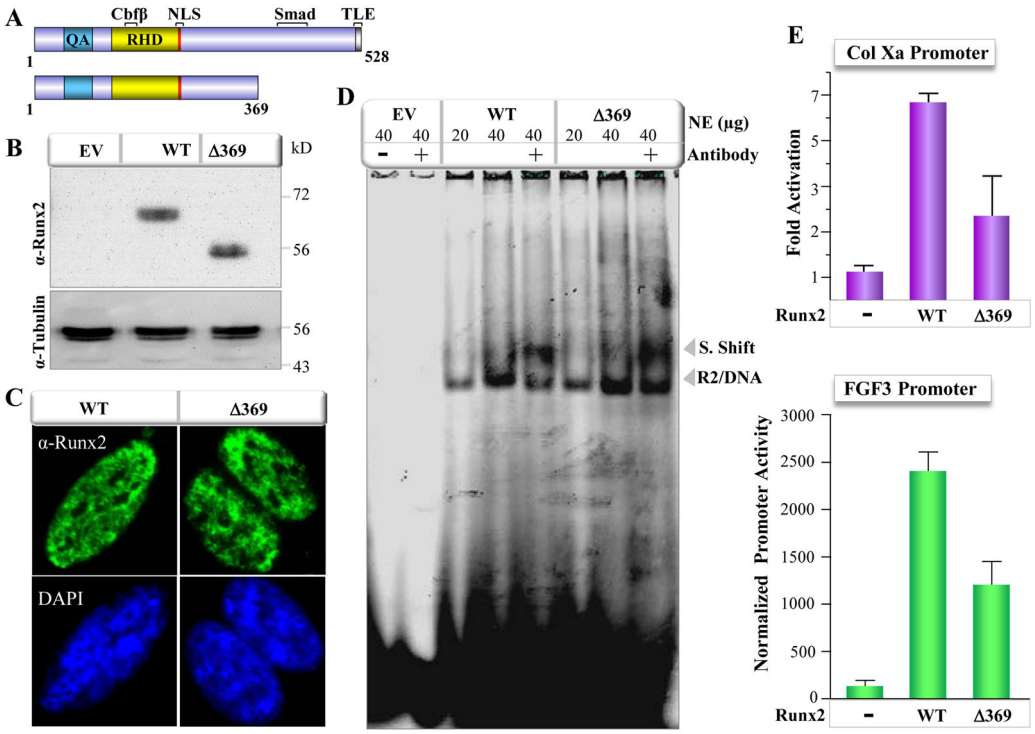


**Figure 5. Runx2 ΔE8 mutant protein maintains normal DNA binding and nuclear distribution but exhibits poor transcriptional activity**

(A) Schematic illustration of key regulatory domains in the wild type Runx2 protein. These include QA (Poly glutamic acid and alanine stretch), RHD (DNA-binding runt homology domain), NLS (nuclear localization signal), Cbfβ and SMAD interaction regions, transcriptional activation and VWRPY repressor domain. The mutant protein lack 159aa at the carboxyl end. (B) GH329 cells transfected with 5μg of either empty vector (EV), WT or Δ369 Runx2 expression plasmids were harvested 36 hours later for SDS-PAGE. Blots were probed with antibodies as indicated. (C) Cells transfected with WT or Δ369 Runx2 expression plasmids were processed for in situ immunofluorescence analysis. Digital images captured at 60X magnification are shown. (D) Nuclear extracts (NE) were prepared from cells transfected with EV, WT or Δ369 Runx2 expression plasmids. EMSA were carried with IRDye700 labeled Runx consensus sequences. The Runx2-DNA complex (R2/DNA) and supershifted antibody-Runx2-DNA complex (S. Shift) are indicated. (E) The Col Xa and FGF3 promoter-Luc vectors were co-transfected with either WT or Δ369 Runx2 expression plasmids. Luciferase activities were determined 24 hours later. Data normalized with Renilla luciferase from three independent experiment with four replicates (n=12) is presented.

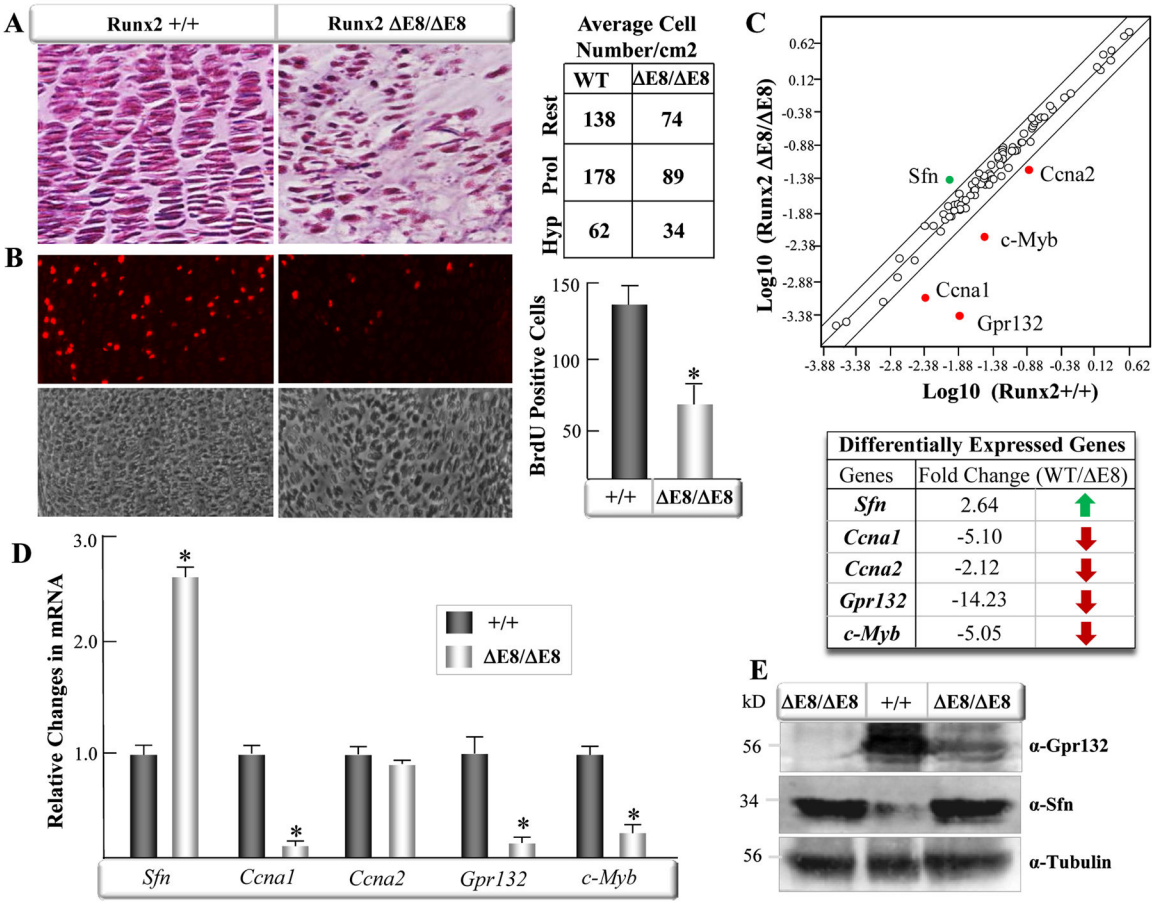


**Figure 6. Runx2 control chondrocyte cell proliferation through a unique set of cell cycle related genes**

(A) Proliferating zone in femoral growth plates of WT and corresponding region in Runx2$^{\Delta E8/\Delta E8}$ is shown at 40X magnification. Three alternate sections covering central part of the WT and mutant femurs were used for cell counting. Four regions in each zone were randomly selected to count cell number per cm$^2$. Pooled data of average cell numbers from 3 WT and 3 mutant femurs are presented in the table. (B) Chondrocyte cell proliferation was assessed by BrdU incorporation at E18.5. Representative image of positive cells in proliferative zone from WT and Runx2$^{\Delta E8/\Delta E8}$ mice are shown. BrdU positive cells were counted per 1000 DAPI positive cells in the growth plate. Pooled data from 3 WT and 3 mutant littermates are presented. Asterisk denote $p<0.05$. (C) RNA from new born WT and Runx2$^{\Delta E8/\Delta E8}$ limbs were isolated. Expression profiles of 84 candidate genes involved in various cell cycle checkpoints were analyzed by Mouse Cell Cycle RT$^2$ Profiler™ PCR array. Scatter plot of over- or underexpressed genes are indicated in green and red circles respectively. Pooled data of fold changes in gene expression from 3 independent arrays is shown in table. (D) Expression analysis of indicated genes by q-PCR in E18.5 limbs of WT and Runx2$^{\Delta E8/\Delta E8}$ mice. Pooled data from 3 WT and 3 mutant mice show significant difference ($p<0.05$). (E) The E18.5 limbs were homogenized for protein analysis. Blots were probed with α-Sfn and Gpr132 antibodies and β-tubulin used as a loading control.

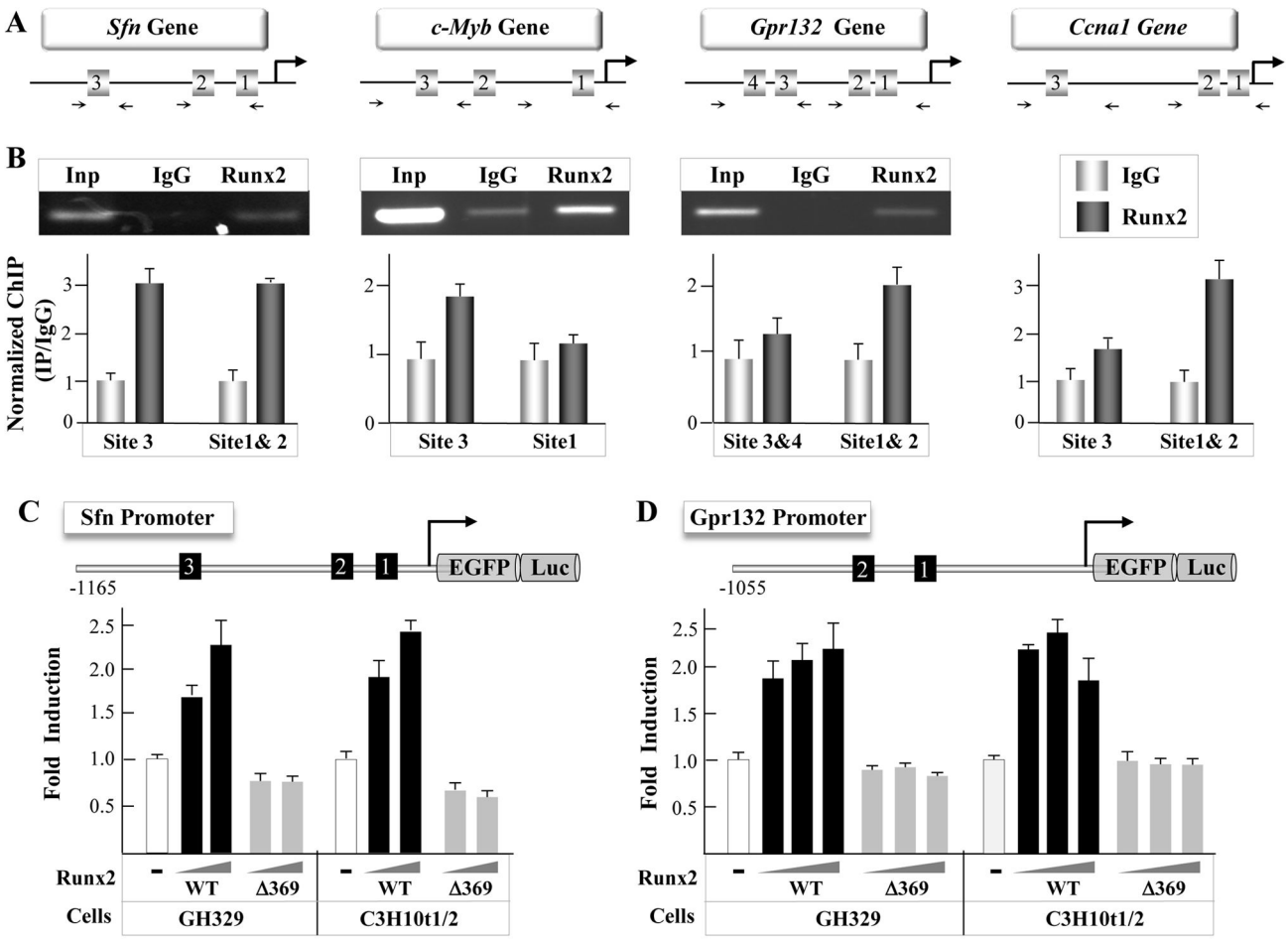


**Figure 7. Runx2 is recruited to Sfn, c-Myb, Gpr132 and Ccna1 gene promoters**

(A) Boxes represent relative positions of multiple RUNX binding sites in indicated promoters. (B) ChIP analysis of Runx2 occupancy at the indicated gene promoters in chondrocytes by PCR and q-PCR. Arrows above indicate the primer pairs in promoter region used for PCR amplification. Amplicons from IgG and Runx2 ChIP samples and 5% input DNA (Inp) were resolved on agarose gel. Relative Runx2 occupancy was calculated with quantitative real time PCR. Average data from three independent ChIP experiments normalized with IgG is presented in graph. (C) Sfn and Gpr132 are direct transcription targets of Runx2 protein. Promoter-reporter plasmid with increasing amount of WT and Δ369 Runx2 expression vectors were co-transfected into indicated cells. Luciferase activities were determined 24hr later and normalized values from 2 independent experiments in triplicates are presented.